Int. J. Heat Mass Transfer. Vol. 15, pp. 741–754. Pergamon Press 1972. Printed in Great Britain

HEAT TRANSFER BY CONDENSATION OF LOW PRESSURE METAL VAPORS

Y. S. HUANG,* F. A. LYMAN† and W. J. LICK

Case Western Reserve University, Cleveland, Ohio, U.S.A.

(*Received* 27 *July* 1971)

Abstract—The film condensation of low pressure metal vapors on isothermal vertical flat plates or tubes is considered. The liquid film is treated as a thin layer in which the acceleration and pressure forces are negligible and across which the temperature distribution is linear. The average behavior of the vapor is found from the linearized one-dimensional vapor flow equations. In order to calculate the rate of condensation, a consistent distribution function for the vapor particles at the liquid–vapor interface is necessary and is determined.

The result of the analysis is a set of algebraic equations from which one can predict the condensation rate of low pressure metal vapors. A large but continuous temperature decrease in the vapor is predicted and calculated. There is good agreement between the most recent and reliable experimental data and the present theoretical calculations if, in the present calculations, the presence of a small amount of a noncondensible gas is included.

NOMENCLATURE

A,	integration constant appearing in equation (2.15);
A_g,	total amount of noncondensible gases per unit area of condensing surface;
a_s,	mean thermal speed;
B,	integration constant appearing in equation (2.16);
C,	molecular speed;
C_1,	integration constant defined by equation (2.11);
C_2,	integration constant defined by equation (2.12);
C_p,	specific heat of vapor or mixture;
C_{pl},	specific heat of condensate;
D_{12},	diffusion coefficient of a mixture of two components;
f,	distribution function of particles at the liquid–vapor interface;
f_1, f_2, f_3,	components of distribution function;
$\bar{G}$,	average mass condensation rate per unit area;
g,	gravitational acceleration;
$\bar{h}$,	average heat transfer coefficient;
$\bar{h}_{Nu}$,	Nusselt's average heat-transfer coefficient;
K,	thermal conductivity of vapor or mixture;
K_l,	thermal conductivity of condensate;
L,	vertical length of condensing surface;
M,	molecular weight;
M_∞,	Mach number of mean vapor flow at infinity;
m,	mass of a molecule;
n_s,	saturation number density at temperature T_s;
n_Δ,	number density of particles of third kind;
P,	pressure of vapor or mixture;
P_i,	pressure of vapor at the interface;
Pr,	Prandtl number;

---

* Presently at Stone & Webster Engineering Corporation, Boston, Massachusetts.

† Presently at Syracuse University, Syracuse, New York.

P_{v_i},	partial pressure of vapor at interface;
P_s,	saturation pressure at temperature T_s;
$\bar{Q}$,	average heat flux per unit area;
R,	universal gas constant;
R_M,	gas constant of vapor or mixture;
r,	radial coordinate;
r_c,	radius of condensing tube;
T,	temperature of vapor or mixture;
T_i,	temperature of vapor at the interface;
T_l,	temperature of condensate;
T_s,	temperature at the liquid–vapor interface;
T_W,	temperature on the wall;
T_Δ,	normal temperature of particles of the third kind;
ΔT_{out},	isentropic temperature drop in outer region;
ΔT_{tot},	total temperature drop;
T',	perturbation of vapor temperature;
U,	molecular velocity in x-direction;
u_l,	velocity of condensate in x-direction;
V,	molecular velocity in y-direction;
v,	velocity of vapor or mixture in y-direction;
$\bar{v}_d$,	mean drift velocity of particles of second kind;
v_i,	velocity of vapor at the interface;
v_l,	velocity of condensate in y-direction;
v',	perturbation of vapor velocity;
W,	concentration or mass fraction of air;
W_i,	concentration or mass fraction of air at the liquid–vapor interface;
x,	direction parallel to condensing surface;
y,	direction normal to condensing surface;
α,	roots defined by equation (2.21);
β_{w_i},	dimensionless parameter defined by equation (3.14);
γ,	ratio of specific heats;
δ_l,	local film thickness of liquid;
$(\delta_l)_e$,	effective film thickness;
λ,	latent heat of condensation;
k,	Boltzmann's constant;
μ,	viscosity of vapor or mixture;
μ_l,	viscosity of condensate;
ν_l,	kinematic viscosity of condensate;
ρ,	density of vapor or mixture;
ρ_i,	density of vapor at the interface;
ρ_l,	density of condensate;
σ,	diameter of molecule;
σ_c,	condensation coefficient;
σ_H,	coefficient defined by equation (2.35).

Subscripts

0,	stagnation conditions;
1,	properties of vapor;
2,	properties of noncondensible gas;
∞,	conditions at infinity or at the intersection of outer and interfacial regions.

Superscripts

0,	zeroth-order solution;
1,	first-order solution.

1. INTRODUCTION

In recent years, liquid metals and metal vapors have been widely used as heat-transfer media in nuclear and spacecraft applications. For the condensation of metal vapors, it has been observed that the measured values of heat-transfer rate fall far below the predictions of Nusselt's theory [1] and its modifications [2–8]. These theories are mainly based upon the assumption that the surface temperature of the liquid is equal to the saturation temperature of the vapor and that the temperature of the vapor is uniform. However, by means of these theories, one can only explain the low observed heat-transfer rates by assuming that the surface temperature of the liquid is much lower than the temperature of the vapor. The classical kinetic theory of condensation [9–13] predicts implicitly a temperature jump at the liquid–vapor interface (within one mean free path of the surface), but the theory still fails to explain the results of experiments. An excellent review of the literature on condensation heat transfer has been prepared by Wilhelm [14].

The inadequacy of Nusselt's theory and the unsatisfactory explanation of the temperature drop at the liquid–vapor interface by the kinetic theory of condensation motivated the present investigation. The physical model studied is that of laminar film condensation of vapor on an isothermal vertical surface.

Details of the film condensation of a pure vapor on an isothermal vertical flat plate are discussed in Section 2. A solution is presented which permits the prediction of the condensation rate of pure vapors or mixtures of a vapor and noncondensible gases. It is shown that, due to the viscosity and thermal conductivity of the vapor, a large temperature drop can exist near the interface in a narrow region whose thickness is proportional to but much larger than the mean free path and inversely proportional to the average Mach number of the condensing vapor. Fairly good agreement between the theory and Sartor's experimental data for condensation of rubidium vapor [15] is obtained.

However, there is rather poor agreement between this theory and Sukhatme's experimental data for condensation of mercury vapor on a finger type condenser [16]. The poor agreement is probably due to the presence of noncondensible gases and in small degree to the isentropic expansion of the vapor itself as it flows radially inward toward the condenser. This vapor expansion was not present in Sartor's essentially constant area one-dimensional flow.

In Section 3, we have extended the theory for pure vapor to include the presence of noncondensible gases. As expected, the presence of noncondensible gases plays a decisive role in retarding the condensation rate of low pressure metal vapors. In Section 4, we have included the additional temperature drop due to the expansion of vapor; this temperature drop may become significant for low pressure systems with high condensation rates especially in the absence of air and other noncondensible gases. The final result of the analysis is good agreement between theory and experiments.

2. FILM CONDENSATION OF A PURE VAPOR ON AN ISOTHERMAL VERTICAL FLAT PLATE

Discussion of the analytical model

For the present problem of film condensation on an isothermal vertical flat plate, it is convenient to divide the vapor flow field into three regions as shown in Fig. 1. In region I, the y-component of the mean velocity of the vapor at infinity is much greater than the maximum value of the x-component of velocity, i.e. the downward velocity at the liquid–vapor interface. For this case, the dynamics of the vapor flow normal to the plate is important and can not be neglected. In region II, the maximum values of the two components of velocity are about the same order of magnitude. In region III, the liquid film plays the important part and the dynamics of the vapor can be completely neglected.

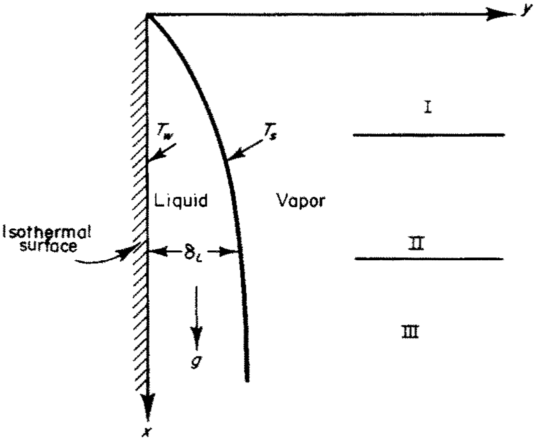

FIG. 1. Schematic of film condensation. In region I, $v_\infty/u_s \gg 1$. In region II, $v_\infty/u_s = O(1)$. In region III, $v_\infty/u_s \ll 1$.

Under conditions of (a) large value of latent heat, (b) long length of condensing plate, and (c) high vapor density, region III will dominate and the temperature change in the vapor may be neglected. These conditions are usually met in condensing steam and organic vapor systems and explain why Nusselt's theory works. On the other hand, the condensation of low pressure metal vapor generally occurs under the following conditions: (a) a smaller value of latent heat, (b) short length of condensing plate, and (c) low vapor density. Under these conditions, the vapor flow is important, and the temperature drop in the vapor can not be neglected.

If a temperature at the liquid–vapor interface is assumed, the liquid film and the vapor can be treated independently. The former is treated as a liquid boundary layer, while the latter is treated as a one-dimensional vapor flow. However, the two problems are really coupled since the temperature and mass flux are assumed to be continuous at the interface. A kinetic theory argument is necessary to determine the condensation rate and hence the interface temperature.

Liquid film

In the analysis of the liquid film, the following assumptions are made: (a) the surface temperature of the liquid film is approximately constant, (b) the condensate flow is laminar, (c) the fluid properties are constant, (d) momentum changes through the condensate are negligible and therefore the viscous force balances the body force, (e) the vapor drag at the interface is neglected, and (f) the temperature distribution in the liquid film is linear.

With these approximations, the solution for the flow in the liquid film is identical to that for Nusselt's theory. The result for $\bar{G}$, the average mass condensation rate per unit area, is

$$\bar{G} = \tfrac{4}{3}\left(\frac{g K_l^3 \rho_l^2}{4\mu_l \lambda^3 L}\right)^{\frac{1}{4}} (T_s - T_W)^{\frac{3}{4}}. \qquad (2.1)$$

The mean heat-transfer rate of condensation per unit area can be calculated from

$$\bar{Q} = \lambda \bar{G}. \qquad (2.2)$$

Vapour flow

The vapor will be treated approximately as a one-dimensional flow. The general analysis may be simplified by use of the following assumptions: (a) the properties of the vapor are constant, (b) the total temperature drop in the vapor is much smaller than the absolute bulk temperature, although it may be much greater than the temperature drop across the liquid film, (c) the Mach number of the mean vapor flow is very small, and (d) the vapor obeys the perfect gas law. The simplified model and coordinate system is sketched in Fig. 2.

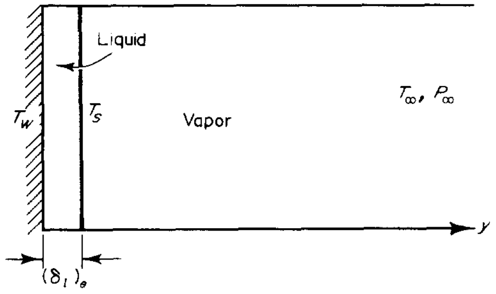

FIG. 2. Schematic of one-dimensional vapor flow.

The governing equations of the vapor flow are the continuity, momentum, energy and state equations and are

$$\frac{\mathrm{d}}{\mathrm{d}y}(\rho v) = 0 \qquad (2.3)$$

$$\rho v \frac{\mathrm{d}v}{\mathrm{d}y} = -\frac{\mathrm{d}P}{\mathrm{d}y} + \tfrac{4}{3}\mu \frac{\mathrm{d}^2 v}{\mathrm{d}y^2} \qquad (2.4)$$

$$\rho v C_p \frac{\mathrm{d}T}{\mathrm{d}y} = K\frac{\mathrm{d}^2 T}{\mathrm{d}y^2} + v\frac{\mathrm{d}P}{\mathrm{d}y} + \tfrac{4}{3}\mu\left(\frac{\mathrm{d}v}{\mathrm{d}y}\right)^2 \qquad (2.5)$$

$$P = \rho R_M T. \qquad (2.6)$$

The appropriate boundary conditions for the vapor are: Bulk vapor conditions ($y \to \infty$),

$$T = T_\infty, \quad P = P_\infty, \quad v = v_\infty = -\frac{\bar{G}}{\rho_\infty} \tag{2.7}$$

where $\bar{G}$ is the mass flux and will be determined from the matching of the vapor and liquid film solutions.

Interface condition ($y = 0$),

$$T = T_s. \tag{2.8}$$

Equations (2.3)–(2.6) may be reduced to the following:

$$-\frac{4}{3}\frac{\mu}{\bar{G}}\frac{dv}{dy} = v + \frac{R_M T}{v} + \frac{C_1}{\bar{G}} \tag{2.9}$$

and

$$-\frac{4}{3}\frac{\mu}{\bar{G}}\frac{dT}{dy}\left(\frac{3}{4}\frac{\gamma}{\gamma - 1}\frac{R_M}{P_r}\right) = \frac{R_M T}{\gamma - 1} - \frac{v^2}{2} - \frac{C_1}{\bar{G}}v - \frac{C_2}{\bar{G}} \tag{2.10}$$

where

$$C_1 = -\bar{G}\left(\frac{P_\infty}{\rho_\infty v_\infty} + v_\infty\right) \tag{2.11}$$

and

$$C_2 = -\bar{G}\left(C_p T_\infty + \frac{v_\infty^2}{2}\right). \tag{2.12}$$

For simplicity, the above system of equations will be linearized. Let $T = T_\infty + T'$ and $v = v_\infty + v'$. By substituting these relations into equations (2.9) and (2.10) and dropping second order terms, one obtains the system,

$$-\frac{4}{3}\frac{\mu}{\bar{G}}\frac{dv'}{dy} = 2v' + \frac{C_1}{\bar{G}}\frac{v'}{v_\infty} + R_M\frac{T'}{v_\infty} \tag{2.13}$$

$$-\frac{4}{3}\frac{\mu}{\bar{G}}\frac{dT'}{dy}\left(\frac{\gamma}{\gamma - 1}\frac{3}{4}\frac{R_M}{P_r}\right) = \frac{R_M}{\gamma - 1}T' - v_\infty v' - \frac{C_1}{\bar{G}}v'. \tag{2.14}$$

The solution may be found by assuming that

$$T' = A\exp\left(-\alpha\frac{3}{4}\frac{\bar{G}}{\mu}y\right) \tag{2.15}$$

$$v' = B\exp\left(-\alpha\frac{3}{4}\frac{\bar{G}}{\mu}y\right) \tag{2.16}$$

where A, B and α are constants. Substitution of equations (2.15) and (2.16) into equations (2.13) and (2.14) leads to

$$(\gamma\alpha - \tfrac{4}{3}P_r)R_M A - \tfrac{4}{3}P_r\frac{\gamma - 1}{\gamma M_\infty^2}v_\infty B = 0 \tag{2.17}$$

$$R_M A + \left[(1 - \alpha) - \frac{1}{\gamma M_\infty^2}\right]v_\infty B = 0 \tag{2.18}$$

where

$$M_\infty^2 = \frac{\rho_\infty v_\infty^2}{\gamma P_\infty}. \tag{2.19}$$

For a nontrivial solution, the determinant of the coefficients of A and B must vanish, i.e.

$$(\tfrac{4}{3}P_r - \gamma\alpha)(1 - \alpha)M_\infty^2 - \tfrac{4}{3}P_r + \alpha = 0. \tag{2.20}$$

The solution when the Prandtl number is two-thirds is presented here. The roots for the limiting case, $M_\infty \to 0$, are

$$\alpha \cong \frac{8}{9}, \qquad -\frac{1}{\gamma M_\infty^2}. \tag{2.21}$$

The positive root is necessary in the present problem. With this value for α, the results for the temperature and velocity distribution are

$$T \cong T_\infty - \left(\frac{T_\infty - T_s}{T_\infty}\right)T_\infty\exp\left(-\frac{2}{3}\frac{\bar{G}}{\mu}y\right) \tag{2.22}$$

$$v \cong v_\infty - \left(\frac{T_\infty - T_s}{T_\infty}\right)v_\infty\exp\left(-\frac{2}{3}\frac{\bar{G}}{\mu}y\right). \tag{2.23}$$

Since $\rho v = \rho_\infty v_\infty$, it follows that

$$\rho \cong \rho_\infty + \left(\frac{T_\infty - T_s}{T_\infty}\right)\rho_\infty\exp\left(-\frac{2}{3}\frac{\bar{G}}{\mu}y\right). \tag{2.24}$$

The pressure may be obtained directly from the equation of state and is

$$P \cong P_\infty - \left(\frac{T_\infty - T_s}{T_\infty}\right)^2 \times P_\infty \left[\exp\left(-\frac{2}{3}\frac{\bar{G}}{\mu}y\right)\right]^2. \qquad (2.25)$$

In this limit of $M_\infty \rightarrow 0$, the linearized solution indicates that the temperature and velocity vary exponentially in a very thin layer near the interface, while the pressure is approximately constant [if $(T_\infty - T_s)/T_\infty \ll 1$]. For a saturated bulk vapor, the vapor at the interface is therefore in a supersaturated condition.

Distribution function

The previous analysis does not permit the calculation of the temperature T_s at the interface. However, this temperature can be determined if one constructs a consistent distribution function which correctly describes the average or macroscopic behavior of the vapor at the interface.

A distribution function is assumed for those particles on the vapor side at the plane which is parallel to and located very close to the interface. The assumed distribution function consists of three parts and is written as

$$f = f_1 + f_2 + f_3\,. \qquad (2.26)$$

f_1 represents particles leaving the liquid with zero drift velocity, f_2 represents particles entering the liquid with a drift velocity $\bar{v}_d$, and f_3 represents particles not entering the liquid but moving over the condensing surface. Since the condensing surface can serve as an energy absorber, the energy normal to the surface may be absorbed and transferred away through the liquid. Hence, for particles of the third kind, the thermal energy normal to the condensing surface may be much smaller than the mean thermal energy.

The forms of f_1, f_2 and f_3 are assumed to be

$$f_1 = n_s\left(\frac{m}{2\pi kT_s}\right)^{\frac{3}{2}} \exp\left(-m\frac{U^2 + V^2 + W^2}{2kT_s}\right)$$

$$f_2 = n_s\left(\frac{m}{2\pi kT_s}\right)^{\frac{3}{2}} \times \exp\left[-m\frac{U^2 + (V - \bar{v}_d)^2 + W^2}{2kT_s}\right]$$

$$f_3 = n_\Delta\left(\frac{m}{2\pi kT_s}\right) \exp\left(-m\frac{U^2 + W^2}{2kT_s}\right) \times \left(\frac{m}{2\pi kT_\Delta}\right)^{\frac{1}{2}} \exp\left(-m\frac{V^2}{2kT_\Delta}\right)$$

where T denotes the normal temperature of particles of the third kind.

If the mean drift velocity of particles of the second kind is much smaller than the mean thermal speed, the equation for f_2 may be simplified to

$$f_2 \cong \left(1 + \frac{2\bar{v}_d}{a_s^2}V\right) f_1 \qquad (2.27)$$

where $a_s^2 = 2kT_s/m$.

The macroscopic properties of the vapor at the interface are calculated from the following definitions for the temperature T_i, the density ρ_i, and the velocity v_i:

$$\tfrac{3}{2}kT_i = \frac{\iiint_{-\infty}^{\infty} \tfrac{1}{2}mC^2 f\,\mathrm{d}U\,\mathrm{d}V\,\mathrm{d}W}{\iiint_{-\infty}^{\infty} f\,\mathrm{d}U\,\mathrm{d}V\,\mathrm{d}W} \qquad (2.28)$$

$$\rho_i = \iiint_{-\infty}^{\infty} mf\,\mathrm{d}U\,\mathrm{d}V\,\mathrm{d}W \qquad (2.29)$$

$$v_i = \frac{\iiint_{-\infty}^{\infty} mVf\,\mathrm{d}U\,\mathrm{d}V\,\mathrm{d}W}{\iiint_{-\infty}^{\infty} mf\,\mathrm{d}U\,\mathrm{d}V\,\mathrm{d}W}. \qquad (2.30)$$

The interface conditions are chosen to be the same as those of the previous analysis, namely, $T_i = T_s$, $P_i \cong P_\infty$, and $\rho_i = P_\infty/R_M T_s$.

By direct integration of equations (2.28)–(2.30) and elimination of n_Δ and $\bar{v}_d$, one obtains the equation

$$P_\infty - P_s = \frac{\bar{G}}{\pi}(2\pi R_M T_s)^{\frac{1}{2}}\left(2 + \frac{T_\Delta/T_s}{1 - T_\Delta/T_s}\right) \quad (2.31)$$

which, when rewritten for the case of $T_\Delta/T_s \to 0$, becomes

$$\bar{G} = \frac{\pi}{2}\frac{P_\infty - P_s}{(2\pi R_M T_s)^{\frac{1}{2}}}. \quad (2.32)$$

It is interesting at this point to compare the present result to that derived from Schrage's [10] or Kucherov–Rikenglaz's analysis [11]. Their result can be written in the simplified form,

$$\bar{G} = \frac{2\sigma_c}{2 - \sigma_c}\frac{P_\infty - P_s}{(2\pi R_M T_\infty)^{\frac{1}{2}}}. \quad (2.33)$$

Equations (2.32) and (2.33) lead to the following formula:

$$\frac{2\sigma_c}{2 - \sigma_c} = \frac{\pi}{2}\left(\frac{T_\infty}{T_s}\right)^{\frac{1}{2}}. \quad (2.34)$$

For a temperature drop in the vapor which is not appreciably large, so that $T_\infty/T_s \doteq 1$, the above equations predict a value of $\sigma_c + 0{\cdot}88$.

The data for condensation of liquid metals [16–25] has been plotted in Fig. 3 (taken from [26]) according to equation (2.33). The equivalent values of $\sigma_c = 0{\cdot}88$–$0{\cdot}92$ from the present theory are shown by the shaded stripe which includes most data at lower pressures up to 0·1 atm. The discrepancy at higher pressures can be explained by either an error analysis [15] or the presence of noncondensible gases.

With the present approximation for the distribution function, an interesting coefficient σ_H may be defined which resembles the usual condensation coefficient; namely σ_H is the fraction of the total number density of particles of the second and third kind that will actually condense, i.e.

$$\sigma_H = \frac{1}{1 + [(P_\infty - P_s)/P_\infty]}. \quad (2.35)$$

In the present problem, σ_H has values between 0·5 and 1·0 and is shown in Fig. 4. When the condensation rate is zero, σ_H is unity and decreases as the condensation rate increases.

Some results for condensation of one dimensional rubidium vapor are shown in Fig. 5, where curves of heat-transfer rate per unit area $\bar{Q}$ vs. the total temperature drop, $T_\infty - T_W$, for different values of vapor pressure P_∞ are plotted. The physical properties of rubidium were taken from [27] and are as follows:

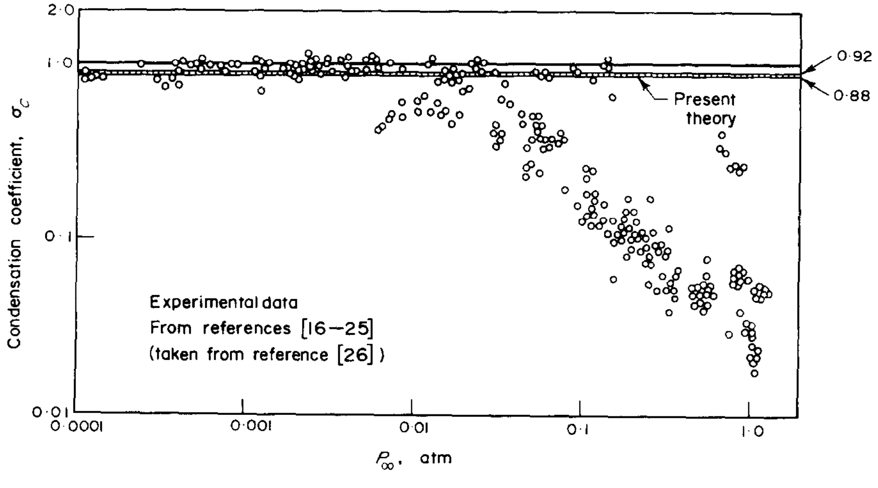

FIG. 3. Condensation coefficient data.

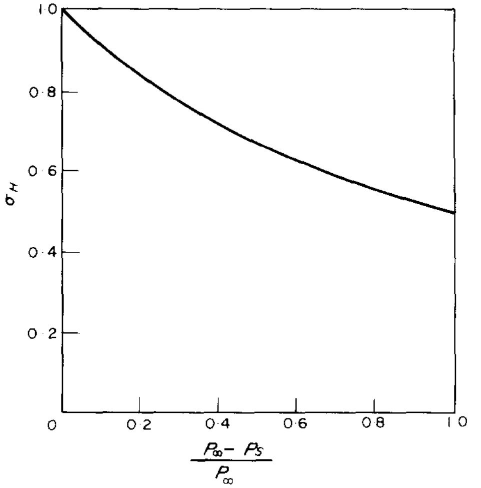

FIG. 4. σ_H vs. $(P \quad - P_s)/P$

$K_l = 23$ Btu/hft°F, $\rho_l = 92$ lbm/ft^3, $C_{pl} = 0{\cdot}0913$ Btu/lbm°F, $\mu_l = 60$ lbm/fth, $\lambda = 381$ Btu/lbm, and $M = 85{\cdot}5$ lbm/mole. The saturation pressure is a function of temperature and was also taken from [27].

In Fig. 5, the theoretical results for various pressures are compared with Sartor's experimental data. Sartor's experiment was essentially a one-dimensional, constant area, vapor flow condensing on a liquid layer of uniform thickness of about 0·12 in. The vapor pressures in his experimental work varied from 1·648 to 8·991 psia. Theoretical results are shown for vapor pressures of 8·991, 1·698, 0·25 and 0·125 psia. As can be seen, lower vapor pressures give lower heat-transfer rates.

It can be shown that the interfacial region across which the temperature drop inside the vapor occurs is very thin. The Mach number in Sartor's experiments with rubidium varied from 0·002 to 0·005. The thickness of the interfacial region is about 500–1000 mean free paths of rubidium vapor, or of the order of 5×10^{-5} in. This confirms Sartor's conclusion that there is a rapid temperature change near the liquid–vapor interface.

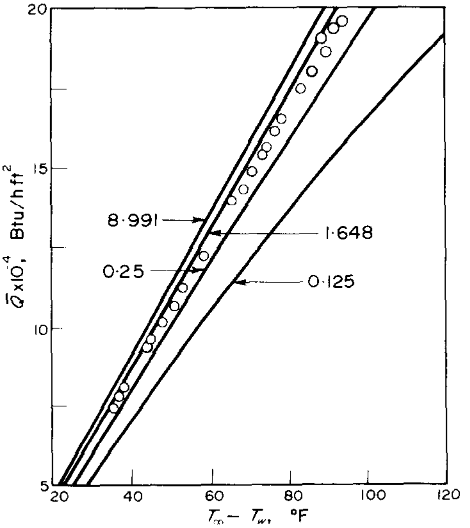

FIG. 5. Comparison of present theory with experimental data (rubidium). The solid lines have been calculated by means of the present theory for values of vapor pressure of 8·991, 1·648, 0·25 and 0·125 psia. ○ denotes Sartor's experimental data obtained for vapor pressures from 1·648 to 8·991 psia.

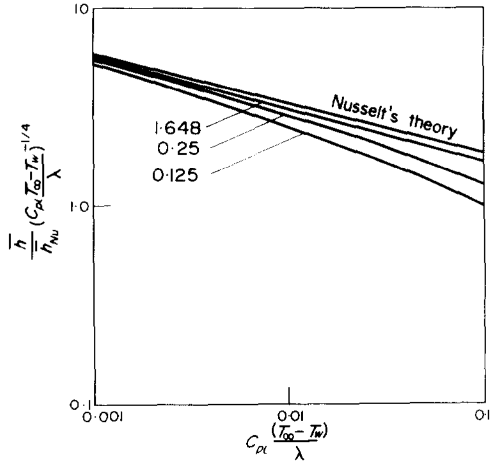

FIG. 6. Comparison of present theory with Nusselt's theory (rubidium). The solid lines have been calculated by means of the present theory for values of vapor pressure of 1·648, 0·25 and 0·125 psia.

As a comparison with Nusselt's theory, the ratio of the average heat transfer coefficients calculated from the present theory and from Nusselt's theory is plotted against the parameter $C_{pl}(T_\infty - T_W)/\lambda$ in Fig. 6. The general trend is that lower vapor pressures give greater deviations from Nusselt's theory.

The agreement between Sartor's data and the theoretical prediction is good with the discrepancy between the two being less than 10 per cent, but more data in a much lower pressure range is needed to justify the theory. Some important experiments of condensation of metal vapors at lower pressures have been conducted on a finger type condenser [16]. The available data shows that the heat flux is considerably smaller than the predictions from the above theory. The discrepancy may be due to the presence of noncondensible gases and to a small degree to the isentropic expansion flow of the vapor itself. These effects are discussed in the following sections.

3. CONSIDERATION OF THE PRESENCE OF NONCONDENSIBLE GASES

The following analysis is restricted to a system composed of a mixture of vapor and air. In experiments on condensing metal vapors, the amount of air is kept as low as possible and therefore in the present analysis the concentration of air may be assumed to be very small. The same physical model shown in Fig. 2 is used here.

The governing equations for a mixture have the same form as equations (2.3)–(2.6) except that the properties are those for a mixture. In the present case, since the concentration of air is assumed to be extremely small, the properties of the mixture are the same as those of the pure vapor to a good approximation.

In addition to equations (2.3)–(2.6), an equation to determine W, the concentration or mass fraction of air, is needed. This equation is

$$\rho v W = \rho D_{12} \frac{dW}{dy} \tag{3.1}$$

which represents the balance between mass convection and mass diffusion. D_{12} is the diffusion coefficient for the mixture. Here and later, subscripts 1 and 2 denote respectively the pure vapor and air. From the kinetic theory for a rigid spherical molecule [28, 29], it can be shown that

$$D_{12} = \frac{3}{8}\sqrt{\frac{\pi}{2}\frac{kT}{P\pi}} - \frac{1}{\left(\frac{\sigma_1 + \sigma_2}{2}\right)^2} \left(\frac{M_1 + M_2}{M_1 M_2} RT\right)^{\frac{1}{2}} \tag{3.2}$$

where σ is the diameter of a molecule. For the present calculations, all properties will be evaluated at the vapor temperature T_∞.

It is convenient to solve the governing equations by means of a perturbation expansion in W_i, where W_i is the local concentration of air at the liquid–vapor interface. Assume an asymptotic expansion in W_i for all dependent variables, i.e. $P = P^{(0)} + W_i P^{(1)} + \ldots$. $W = W_i W^{(1)} + \ldots$ etc. The zeroth order solution is then just the solution in the absence of any air.

By substituting these expansions into equations (2.3)–(2.6) and (3.1) and retaining terms of lowest order in W_i, one obtains a system of equations identical to that in Section 2 and a diffusion equation

$$\rho^{(0)} v^{(0)} W^{(1)} = \rho^{(0)} D_{12} \frac{dW^{(1)}}{dy}. \tag{3.3}$$

By neglecting the small variation of the density, one can rewrite this equation as

$$\bar{G} W^{(1)} = -\rho_\infty D_{12} \frac{dW^{(1)}}{dy} \tag{3.4}$$

for which the boundary condition is $W^{(1)} = 1$ at $y = 0$ and $W^{(1)} \to 0$ as $y \to \infty$. The concentration can then be found by integrating the above equation and is

$$W^{(1)} = \exp\left(-\frac{\bar{G}}{\rho_\infty D_{12}} y\right). \tag{3.5}$$

Since D_{12} is about the same order of magnitude as v_1, the thickness of the diffusion layer is found to be comparable to that of a visco-conduction layer.

To calculate W_i, the total amount of air per unit area A_g must be specified, where

$$A_g = \int_0^\infty \rho_\infty W_i \exp\left(-\frac{\bar{G}y}{\rho_\infty D_{12}}\right) dy. \quad (3.6)$$

After integration of this equation, one obtains

$$W_i = \frac{A_g \bar{G}}{\rho_\infty D_{12}}. \quad (3.7)$$

As can be seen, for a fixed amount of air A_g and rate of condensation $\bar{G}$, as the vapor density decreases the concentration of air at the interface increases. This will seriously retard the rate of mass condensation and explains the significance of the presence of non-condensible gases in a low pressure metal vapor heat transfer system. These effects will be discussed in more detail in the following section.

The partial pressure of vapor P_{v_i} at the interface is calculated from

$$P_{v_i} \cong P_\infty \frac{1 - W_i}{1 - [1 - (M_1/M_2)]W_i}. \quad (3.8)$$

By letting

$$\beta_{W_i} = \frac{1 - W_i}{1 - [1 - (M_1/M_2)]W_i} \quad (3.9)$$

one can write the mass flux for a mixture as

$$\bar{G} = \frac{\pi}{2} \frac{\beta_{W_i} P_\infty - P_s}{(2\pi R_{M_1} T_s)^{\frac{1}{2}}}, \quad (3.10)$$

in contrast to equation (2.32) which was obtained for the case of a pure vapor.

4. FILM CONDENSATION ON THE OUTSIDE OF AN ISOTHERMAL VERTICAL TUBE

Theory

The condensation of low pressure metal vapor on a finger type condenser is illustrated in Fig. 7. It is convenient to define three regions in the flow field: (1) the outer region in which the vapor expands isentropically, (2) the interfacial region in which the vapor is slowed down and cooled by the presence of noncondensible gases and by viscosity and heat resistance, and (3) the liquid film.

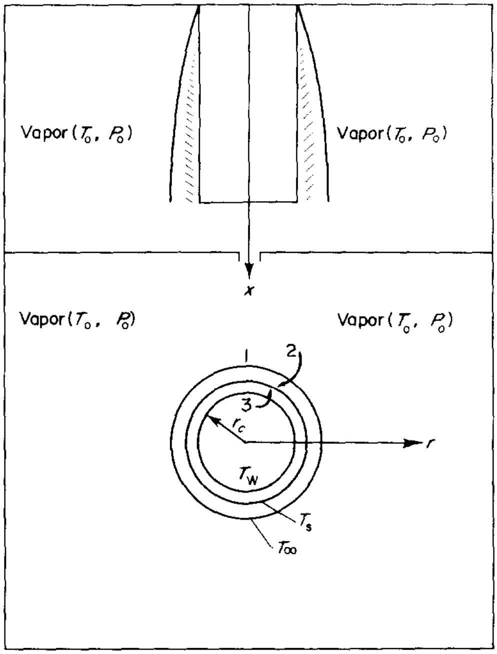

FIG. 7. Schematic of finger type condenser. Regions 1, 2 and 3 are the outer, interfacial, and liquid film regions respectively.

Since the thickness of the liquid film and the interfacial region are very thin compared to the radius of the condensing tube, the flow problem in these two regions can be treated in the same way as that for a vertical flat plate. The general analysis and results in Sections 2 and 3 can then be applied here. In the outer region, the flow field and the temperature drop can be found by approximating the flow as a one-dimensional radial flow of an inviscid pure vapor. The reason for considering the vapor pure is that almost all of the noncondensible gas is in the interfacial region.

In the outer region, from the solution for isentropic radial flow, the mass flux is

$$\bar{G} = \rho_0 \left\{ \frac{2\gamma R_M T_0}{\gamma - 1} \left[\left(\frac{P_\infty}{P_0}\right)^{2/\gamma} - \left(\frac{P_\infty}{P_0}\right)^{(\gamma+1)/\gamma} \right] \right\}^{\frac{1}{2}}. \quad (4.1)$$

Table 1. Temperature drop in the outer, interfacial, and liquid film regions, including the presence of air. Points A, B and C refer to corresponding points in Fig. 8

Stagnation pressure (P_0)	Point	Temperature drop (°F) Outer region Isentropic	 Saturation	 Interfacial region Isentropic	 Saturation	 Liquid film region
	A	2	0·4	19·5	21·1	0·4
0·05 psia	B	8	1·2	46	52·8	1·05
	C	14	2·5	80·5	92·0	1·5
	A	2	0·3	21·5	23·3	2·6
0·15 psia	B	8	1·0	58·5	65·5	4·5
	C	16	2·2	117	130·8	7·2
	A	1·5	0·2	18·5	19·8	2·7
0·25 psia	B	4	0·8	37	40·2	5
	C	16	3·0	113	126·0	14

The mass flux in the liquid film and interfacial regions can be found from equations (2.1) and (3.10), respectively.

Results

Some detailed results of analytical computations based upon Sukhatme's experimental conditions for mercury are presented in Table 1 and Fig. 8. The length of the condensing tube was chosen to be 6 in., while the properties of mercury were taken from [30] and [31] and are as follows: $C_{pl} = 0{\cdot}033$ Btu/lbm°F, $\rho_l = 830$ lbm/ft^3, $\nu_l = 0{\cdot}1 \times 10^{-5}$ ft^2/s, $K_l = 6{\cdot}64$ Btu/hft°F, $\lambda = 127$ Btu/lbm and $M = 201$ lbm/mole. The saturation pressure is a function of temperature and was taken from [31]. To get agreement with Sukhatme's data, it is necessary to assume there is $4{\cdot}9 \times 10^{-9}$ lbm of air present in his chamber, the dimensions of which are 6 in. dia. and 11 in. length. The corresponding vacuum pressure of air is $4{\cdot}94 \times 10^{-6}$ bars. In Fig. 8, the letters A, B and C refer to points for which the temperature drops in various regions have been listed in Table 1. As can be seen from Table 1, the temperature drop in the outer and liquid film regions is negligible compared to that in the interfacial region. Also shown in Table 1 are the changes in saturation temperature for the various points in Fig. 8. Note that the saturation temperature changes are smaller than the isentropic temperature changes.

In the absence of air but under the same conditions as above, the theoretical predictions of heat flux are about two times higher than Suihatme's data. In this case, as the heat flux increases, the temperature drop in the outer region may become comparable to or even more important than that in the interfacial region. Generally speaking, the relative importance of the isentropic temperature drop in the outer region depends heavily upon the presence of air. The presence of air will decrease the heat flux as well as the temperature drop in the outer region and, on the other hand, will increase

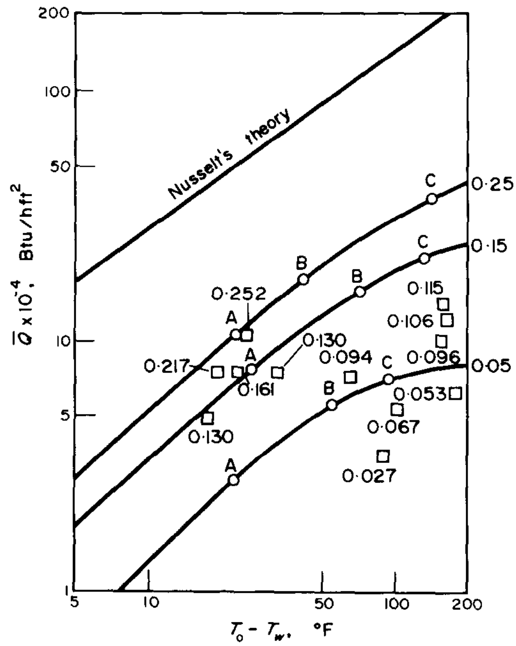

FIG. 8. Comparison of experimental data with the present theory including the presence of air. The solid lines have been calculated by means of the present theory for vapor pressures of 0·05, 0·15 and 0·25 psia. □ denotes Sukhatme's experimental data for mercury with numbers denoting vapor pressures in psia. The temperature drops within the various regions have been calculated for points A, B and C (see Table 1).

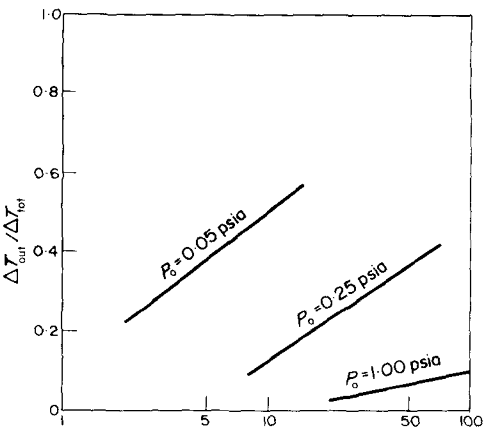

FIG. 9. Fraction of the isentropic temperature drop in the outer region for mercury vapor in the absence of air.

substantially the temperature drop in the interfacial region. To show the dependence of the temperature drop in the outer region on the heat flux, the ratio of ΔT_{out} to ΔT_{tot} is plotted against the heat flux $\bar{Q}$ in Fig. 9, in which the absence of air is assumed.

5. DISCUSSION AND CONCLUSIONS

A set of algebraic equations has been found for the prediction of heat-transfer rate by condensation. Good agreement has been found between the available data and the theoretical predictions when the presence of a small amount of air was considered.

The theory is limited to small values of $(T_\infty - T_s)/T_\infty$ and Mach number of the mean vapor flow, but it can be extended to larger values of these parameters by numerical solutions of the basic equations. However, a good heat-transfer system transfers heat with temperature drops as small as possible. The corresponding Mach number is accordingly very small. Typically, the values of $(T_\infty - T_s)/T_\infty$ are 0·05 or less and the values of Mach number are 0·2 or less. For these limits, the error involved in using the linearized analysis may be estimated to be 4 per cent or less, and therefore the linearized solution is a good approximation.

The approximation of a constant temperature on the surface of the liquid film was validated by Sukhatme's experiment. He measured the thickness distribution of the liquid film and found that it could be described by Nusselt's analysis with an assumed constant film surface temperature.

Only the solution for small concentration of noncondensible gases was given in this investigation. It was found that the presence of noncondensible gases seriously retards the heat-transfer rate of condensation. In experiments, a great deal of care was taken to keep the amount of noncondensible gases small. For this reason, the solution for small concentration is sufficient for comparison of theory and experiment. In the calculations, the concentration of air at the liquid–vapor interface is 0·1 or less, which is small.

The effect of free convection was considered by retaining the body force term in the momentum equation. It was found that free convection decreases the heat-transfer rate slightly, but the correction was small, about 0·1 per cent or less. For a small temperature drop, free convection is apparently not important, while for a large temperature drop, the motion due to free convection is still far less important than the induced mean vapor flow.

There are other factors not being considered in the present analysis, for instance, the impurity of the vapor, the contamination of the liquid surface, surface tension, and possible nucleation of the vapor near the interface. Intuitively all these factors probably decrease condensation heat transfer. We conclude that the present theory can be used in predicting an upper limit of heat-transfer rate due to condensation of low pressure metal vapors.

ACKNOWLEDGEMENTS

The authors would like to thank Professor Warren M. Rohsenow for his suggestions and critical review of the manuscript.

This research was supported by the National Aeronautics and Space Administration under Grant NGR-36-003-064.

REFERENCES

1. W. Nusselt, *Z. Ver. Deutsch.* **60**, 541 (1916).
2. L. A. Bromley, *Ind. Engng Chem.* **44**, 2966 (1952).
3. R. A. Seban, Remarks on film condensation with turbulent flow, *Trans. Am. Soc. Mech. Engrs* **76**, 299–303 (1954).
4. W. M. Rohsenow, Heat transfer and temperature distribution in laminar-film condensation, *Trans. Am. Soc. Mech. Engrs* **78**, 1645–1648 (1956).
5. E. M. Sparrow and J. L. Gregg, A boundary layer treatment of laminar-film condensation, *J. Heat Transfer* **81C**, 13–18 (1959).
6. M. M. Chen, An analytical study of laminar film condensation: Part I—Flat plates, *J. Heat Transfer* **83C**, 48–54 (1961).
7. J. C. Y. Koh, E. M. Sparrow and J. P. Hartnett, *Int. J. Heat Mass Transfer* **2**, 69 (1961).
8. J. C. Y. Koh, An integral treatment of two-phase boundary layer in film condensation, *J. Heat Transfer* **83C**, 359–362 (1961).
9. H. Hertz, *Ann. Phys. Chem., Poggendorf* **17**, 193–200 (1882).
10. R. W. Schrage, *A Theoretical Study of Interface Mass Transfer*. Columbia University Press, New York, N.Y. (1953).
11. R. Y. Kucherov and L. E. Rikenglaz, *Zh. Eksperim. Teor. Fiz.* **37**(1), 7 (1959).
12. D. A. Labuntsov, An analysis of evaporation and condensation process, *High Temperature* **5**(4), 579 (1967).
13. A. J. Patton and G. S. Springer, A kinetic theory description of liquid–vapor phase change, Sixth Rarefied Gas Dynamics Conference (1968).
14. D. J. Wilhelm, Condensation of metal vapors: mercury and the kinetic theory of condensation, Argonne National Laboratory report ANL-6948 (1964).
15. A. J. Sartor, R. E. Balzhiser and R. E. Barry, Condensing heat transfer considerations relevant to rubidium and other alkali metals, Eleventh National Heat Transfer Conference, A.I.Ch.E., Preprint 5 (1969).
16. S. P. Sukhatme and W. M. Rohsenow, Heat transfer during film condensation of a liquid metal vapor, *J. Heat Transfer* **88C**, 19–28 (1966).
17. P. M. Meyrial, M. L. Morin and W. M. Rohsenow, Heat transfer during film condensation of potassium vapor on a horizontal plate, Report No. 70008-52, Heat Transfer Laboratory, M.I.T. (1968).
18. V. I. Subbotin, N. V. Bakulin, M. N. Ivanoskii and V. P. Sorokin, *Teplofiz. Vysok. Temp.* **5**, (1967).
19. S. J. Wilcox and W. M. Rohsenow, Film condensation of liquid metals—precision of measurement, Report No. 71475-62, Heat Transfer Laboratory, M.I.T. (1969).
20. V. I. Subbotin, M. N. Ivanovskii, V. P. Sorokin and V. A. Chulkov, *Teplofiz. Vysok. Temp.* **4**, 616 (1964).
21. D. G. Kroger and W. M. Rohsenow, Film condensation of saturated potassium vapor. *Int. J. Heat Mass Transfer* **10**, (1967).
22. V. I. Subbotin, M. N. Ivanovskii and A. I. Milovanov, Condensation coefficient for mercury, *Atomn. Energ.* **24**(2), (1968).
23. B. Misra and C. F. Bonilla, Heat transfer in the condensation of metal vapors: mercury and sodium up to atmospheric pressure, *Chem. Engng Prog. Symp. Ser.* **52**(7), 18 (1965).
24. R. E. Barry and R. E. Balzhiser, Condensation of sodium at high heat fluxes, Proc. 3rd Int. Heat Transfer Conf., **2**, 318, Chicago, Illinois (1966).
25. I. T. Aladyev, N. S. Kondratyev, V. A. Mukhin, M. E. Mukhin, M. E. Kipshidze, I. Parfentyev and J. V. Kisselev, Film condensation of sodium and potassium vapor, 3rd Int. Heat Transfer Conf., Vol. 2, p. 313, Chicago, Illinois (1966).
26. P. M. Meyrial, M. M. Morin, S. J. Wilcox and W. M. Rohsenow, Effect of precision of measurement on reported coefficients for liquid metals, 4th Int. Heat Transfer Conf., Versailles (September 1970).
27. *Liquid–Metals Handbook*. Atomic Energy Commission (June 1952).
28. E. H. Kennard, *Kinetic Theory of Gases*. McGraw-Hill, New York (1938).
29. S. Chapman and T. C. Cowling, *The Mathematical Theory of Non-uniform Gases*. Cambridge Press (1953).
30. E. R. G. Eckert and R. M. Drake, Jr., *Heat and Mass Transfer*. McGraw-Hill, New York (1959).
31. J. E. Lay, *Thermodynamics*. Charles E. Merrill, Columbus, Ohio (1964).

TRANSFERT THERMIQUE PAR CONDENSATION DE VAPEURS MÉTALLIQUES À BASSE PRESSION

Résumé—On considère la condensation en film de vapeurs métalliques à basse pression sur des plaques planes verticales et isothermes ou sur des tubes. On traite le film liquide comme une couche mince dans laquelle les forces d'inertie et de pression sont négligeables et à travers laquelle la distribution de température est linéaire. Le comportement moyen de la vapeur est trouvé à partir d'équations linéarisées et monodimensionnelles de l'écoulement de vapeur. Afin de calculer le débit de condensation, on détermine une fonction de distribution pour les particules de vapeur à l'interface liquide-vapeur.

L'analyse conduit à un système d'équations algébriques à partir desquelles on peut prédire le débit de condensation de vapeur métallique à basse pression. Une décroissance de température étendue et continue dans la vapeur est démontrée par le calcul. Il y a bon accord entre les résultats experimentaux les plus récents et ces calculs théoriques si dans ces derniers la présence d'une petite quantité de gaz non condensable est prise en compte.

WÄRMEÜBERGANG BEI DER KONDENSATION VON METALLDÄMPFEN GERINGEN DRUCKS

Zusammenfassung—In diesem Beitrag wird die Filmkondensation von Metalldämpfen bei niedrigen Drücken an vertikalen, ebenen Flächen oder an Rohren behandelt. Der Flüssigkeitsfilm wird als dünne Schicht betrachtet, in der Beschleunigungs- and Druckkräfte vernachlässigbar sind und die Temperaturverteilung linear ist. Das durchschnittliche Verhalten des Dampfes wird beschrieben durch die linearisierte, eindimensionale Strömungsgleichung des Dampfes. Um die Kondensationsrate berechnen zu können, ist eine konsistente Verteilungsfunktion der Dampfteilchen an der Phasentrennfläche nötig. Diese Funktion wurde bestimmt.

Das Ergebnis der Untersuchung ist ein Satz algebraischer Gleichungen, mit denen die Kondensationsrate von Metalldämpfen bei niedrigen Drücken vorausberechnet werden kann. Ein grosser, aber stetiger Temperaturabfall im Dampf wird berechnet. Die Übereinstimmung zwischen den neuesten, verlässlichen Experimenten und der hier angeführten theoretischen Berechnung ist gut, wenn in der Berechnung die Gegenwart einer Menge nicht kondensierbaren Gases berücksichtigt wird.

ТЕПЛООБМЕН ПРИ КОНДЕНСАЦИИ ПАРОВ МЕТАЛЛОВ ПРИ НИЗКИХ ДАВЛЕНИЯХ

Аннотация—Рассматривается конденсация паров металлов при низких давлениях на вертикальных изотермических плоских пластинах или трубах. Пленка жидкости рассматривается как тонкий слой, в котором силами ускорения и давления можно пренебречь, а распределение температуры является линейным. Средние характеристики пара находятся из линеаризованных уравнений для одномерного течения пара. Определяется согласованная функция распределения для частиц пара на поверхности раздела жидкость-пар, необходимая для расчета скорости конденсации.

В результате анализа получена система алгебраических уравнений, которые позволяют рассчитать скорость конденсации паров металлов при низких давлениях. Предсказано и рассчитано значительное, но непрерывное понижение температуры. Наблюдается хорошее соответствие между надежными новейшими экспериментальными данными и результатами настоящено анализа при условии, что в данных расчетах учитывается наличие небольшого количества неконденсирующегося газа.